

# Efficient and photostable CsPbI<sub>2</sub>Br solar cells realized by adding PMMA

Yanbo Shang<sup>1,‡</sup>, Zhimin Fang<sup>1,2,‡</sup>, Wanpei Hu<sup>1</sup>, Chuantian Zuo<sup>2</sup>, Bairu Li<sup>1</sup>, Xingcheng Li<sup>1</sup>, Mingtai Wang<sup>3</sup>, Liming Ding<sup>2,†</sup>, and Shangfeng Yang<sup>1,†</sup>

<sup>1</sup>Hefei National Laboratory for Physical Sciences at Microscale, Key Laboratory of Materials for Energy Conversion (CAS), Anhui Laboratory of Advanced Photon Science and Technology, Department of Materials Science and Engineering, University of Science and Technology of China, Hefei 230026, China

<sup>2</sup>Center for Excellence in Nanoscience (CAS), Key Laboratory of Nanosystem and Hierarchical Fabrication (CAS), National Center for Nanoscience and Technology, Beijing 100190, China

<sup>3</sup>Institute of Solid State Physics, Chinese Academy of Sciences, Hefei 230031, China

**Citation:** Y B Shang, Z M Fang, W P Hu, C T Zuo, B R Li, X C Li, M T Wang, L M Ding, and S F Yang, Efficient and photostable CsPbI<sub>2</sub>Br solar cells realized by adding PMMA[J]. *J. Semicond.*, 2021, 42(5), 050501. <http://doi.org/10.1088/1674-4926/42/5/050501>

Organic–inorganic hybrid perovskite materials demonstrate promising applications in high-efficiency perovskite solar cells (PSCs) with a certified power conversion efficiency (PCE) of 25.5% (<https://www.nrel.gov/pv/cell-efficiency.html>). However, intrinsically volatile and thermally unstable nature of the organic cations result in poor thermal stability of organic–inorganic hybrid perovskite materials, hampering the commercialization of organic-inorganic hybrid PSCs<sup>[1]</sup>. All-inorganic CsPbI<sub>3-x</sub>Br<sub>x</sub> ( $x = 0-3$ ) perovskites have been attracting great attention in recent years because of their higher thermal stability<sup>[2]</sup>. Among the reported CsPbI<sub>3-x</sub>Br<sub>x</sub> perovskites, CsPbI<sub>2</sub>Br bears a reasonable balance between bandgap and phase stability, thus becomes the most extensively studied material<sup>[3-15]</sup>. Though there are many works aiming at achieving high-efficiency CsPbI<sub>2</sub>Br PSCs, improving the photostability of CsPbI<sub>2</sub>Br PSCs is another key for commercialization of all-inorganic PSCs. Intriguingly, it has been reported that CsPbI<sub>2</sub>Br is susceptible to make light-induced phase segregation, i.e. severe segregation of CsPbI<sub>2</sub>Br to low-bandgap I-rich and wide-bandgap Br-rich domains *via* ion diffusion, leading to obvious current–voltage hysteresis and decrease of stabilized power output (SPO)<sup>[16-20]</sup>. Such a light-induced phase segregation can be suppressed by optimizing the interface between perovskite layer and charge-transport layer<sup>[18, 19]</sup>. For example, Tian *et al.* improved the photostability of CsPbI<sub>2</sub>Br PSCs through modifying SnO<sub>2</sub> electron-transport layer by PN4N and incorporating dopant-free PDCBT hole-transport layer<sup>[18]</sup>. Xiao *et al.* developed a new dopant-free hole-transport layer PSQ2 to substitute Spiro-OMeTAD, and found that PSQ2-based devices had less SPO loss<sup>[19]</sup>. Despite of the effectiveness of suppressing light-induced phase segregation *via* such interfacial modification, whether the phase segregation is induced merely by light illumination or already exists in the crystallization of CsPbI<sub>2</sub>Br remains unclear yet. Another open question is whether the photostability of CsPbI<sub>2</sub>Br can be improved by eliminating light-induced phase segrega-

tion of CsPbI<sub>2</sub>Br *via* modulating the crystallization process of CsPbI<sub>2</sub>Br.

Here, we introduced poly(methyl methacrylate) (PMMA) additive into CsPbI<sub>2</sub>Br to modulate the crystallization process of perovskite films. We found that phase segregation occurs during crystallization of CsPbI<sub>2</sub>Br especially under fast crystallization rate and low annealing temperature, and this intrinsic phase segregation exacerbates light-induced phase segregation. With PMMA additive, CsPbI<sub>2</sub>Br solar cells gave an enhanced PCE of 15.88%, and the photostability was improved.

We added PMMA *via* anti-solvent dripping (Fig. S1)<sup>[21]</sup>. The CsPbI<sub>2</sub>Br film with PMMA exhibited slow color change from transparent to brown-yellow during annealing (Fig. S2), indicating that PMMA incorporation leads to slower crystallization of CsPbI<sub>2</sub>Br and larger grain with reduced root-mean-square (RMS) roughness. (Fig. 1(a), Figs. S3 and S4). The crystallinity and crystalline orientation of CsPbI<sub>2</sub>Br film were also optimized. XRD shows that CsPbI<sub>2</sub>Br film with 0.05 mg/mL PMMA has strongest (100) and (200) diffraction peaks (Fig. S5). The GIXRD patterns reveal the improved orientation of CsPbI<sub>2</sub>Br crystal with (100) and (200) planes parallel to the substrate (Figs. S6 and S7). PMMA incorporation improves the crystalline orientation of CsPbI<sub>2</sub>Br along plane (100) (Fig. 1(b)).

We studied the trap-state density ( $n_t$ ) of CsPbI<sub>2</sub>Br layer by using space charge limited current (SCLC) method based on an electron-only device with a structure of ITO/SnO<sub>2</sub>/ZnO/perovskite/PCBM/Ag (Fig. 1(c))<sup>[22]</sup>.  $n_t$  can be calculated by equation:

$$n_t = \frac{2\epsilon\epsilon_0}{eL^2} \times V_{\text{TFL}},$$

where  $\epsilon_0$  is the vacuum permittivity,  $\epsilon$  is the relative dielectric constant of CsPbI<sub>2</sub>Br<sup>[13]</sup>,  $e$  is the elementary charge, and  $L$  is the thickness of perovskite film. The trap-filled limit voltage ( $V_{\text{TFL}}$ ) is the bias voltage at the kink point. The  $n_t$  decreased from  $1.09 \times 10^{16}$  to  $8.18 \times 10^{15}$  cm<sup>-3</sup> after PMMA incorporation. Low trap density favors to reduce charge recombination. The carrier lifetimes ( $\tau$ ) of CsPbI<sub>2</sub>Br films measured by time-resolved photoluminescence (TRPL) were 6.68 and 10.34 ns for the control film and the film with PMMA, respectively (Fig. S8, Table S1)<sup>[23]</sup>. The prolonged carrier lifetime sug-

Yanbo Shang and Zhimin Fang contributed equally to this work.

Correspondence to: L M Ding, [ding@nanoctr.cn](mailto:ding@nanoctr.cn); S F Yang,

[sfyang@ustc.edu.cn](mailto:sfyang@ustc.edu.cn)

Received 24 FEBRUARY 2021.

©2021 Chinese Institute of Electronics

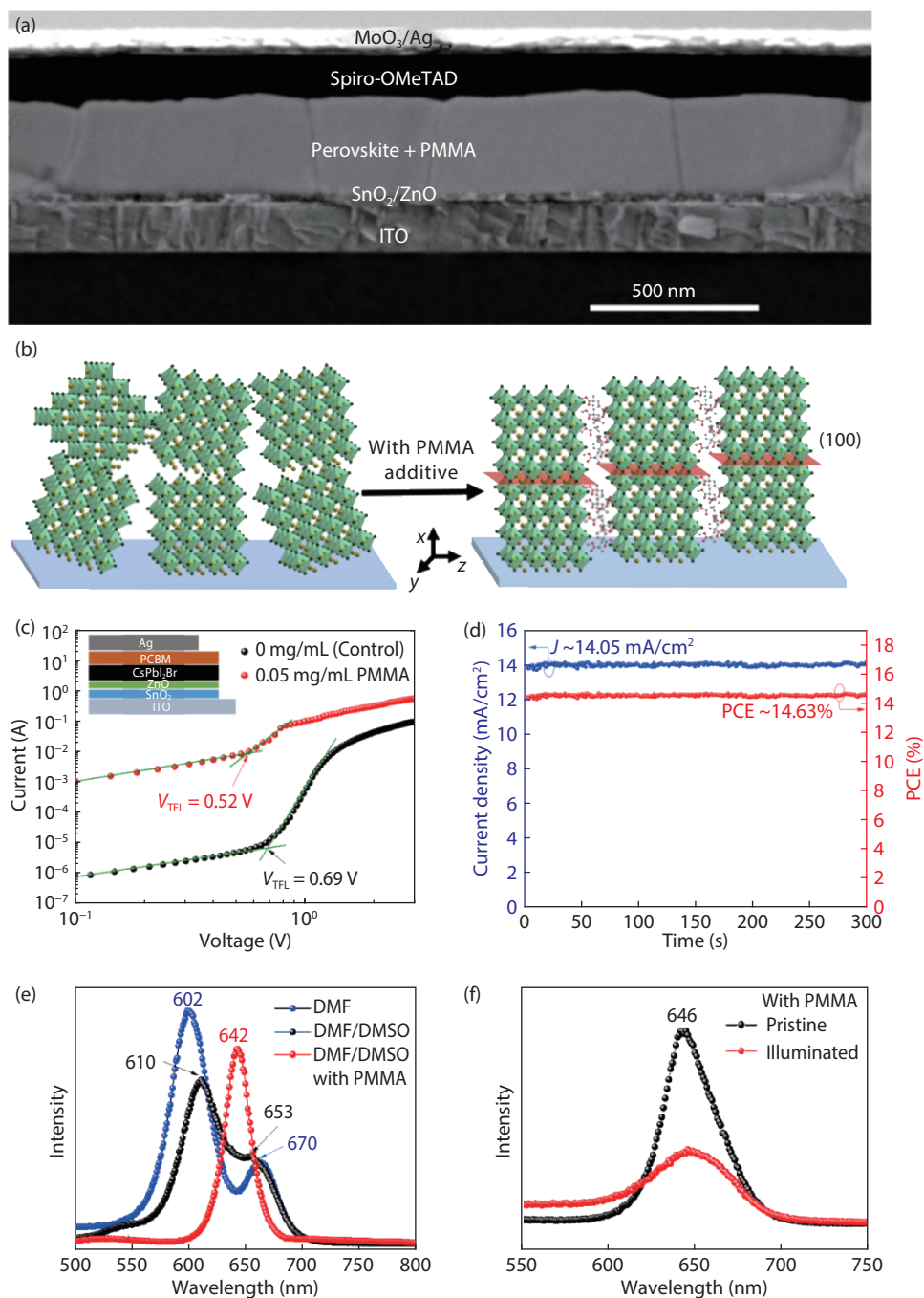


Fig. 1. (Color online) (a) Cross-section SEM image for CsPbI<sub>2</sub>Br solar cell. (b) Schematic illustration of perovskite crystal with and without PMMA. (c) Dark current–voltage curves for the electron-only devices with and without PMMA. (d) Stabilized power output (SPO) of CsPbI<sub>2</sub>Br device with PMMA. (e) Steady-state PL spectra for CsPbI<sub>2</sub>Br films from different fabrication process (annealed at 100 °C). (f) Steady-state PL spectra for CsPbI<sub>2</sub>Br films with PMMA before and after illumination.

gests that PMMA can passivate trap states. The higher intensity of the PL peak for CsPbI<sub>2</sub>Br film (Fig. S9), smaller ideal factor ( $\epsilon$ ) obtained from  $V_{oc}$  vs light intensity plots (Fig. S10), and decreased  $R_{ct}$  (charge transfer resistance) obtained from EIS (Fig. S11 and Table S2) all suggest suppressed non-radiative decay in CsPbI<sub>2</sub>Br film with PMMA.

PSCs with a structure of ITO/SnO<sub>2</sub>/ZnO/CsPbI<sub>2</sub>Br/Spiro-OMeTAD/MoO<sub>3</sub>/Ag were made. The photovoltaic performances for the devices with and without PMMA were compared (Fig. S12, Fig. S13 and Table S3). The PCE increased from 14.42% to 15.88% after adding 0.05 mg/mL PMMA. The negligible change of  $J_{sc}$  is verified by external quantum effi-

ciency (EQE) measurements (Fig. S14). The PCE enhancement for the device with PMMA results from the increases of  $V_{oc}$  (1.124 to 1.216 V) and FF (67.77% to 75.28%), which can be attributed to decreased trap states in CsPbI<sub>2</sub>Br film with PMMA. The devices with PMMA have smaller hysteresis index (Fig. S15 and Table S4) and less degradation of SPO (Fig. 1(d) and Fig. S16(a))<sup>[18, 19]</sup>. The existence of hysteresis and SPO degradation suggest the occurrence of light-induced phase segregation of CsPbI<sub>2</sub>Br<sup>[19, 20]</sup>. The smaller hysteresis and SPO degradation suggest that PMMA can suppress light-induced phase segregation of CsPbI<sub>2</sub>Br.

Without PMMA, the phase segregation of CsPbI<sub>2</sub>Br takes

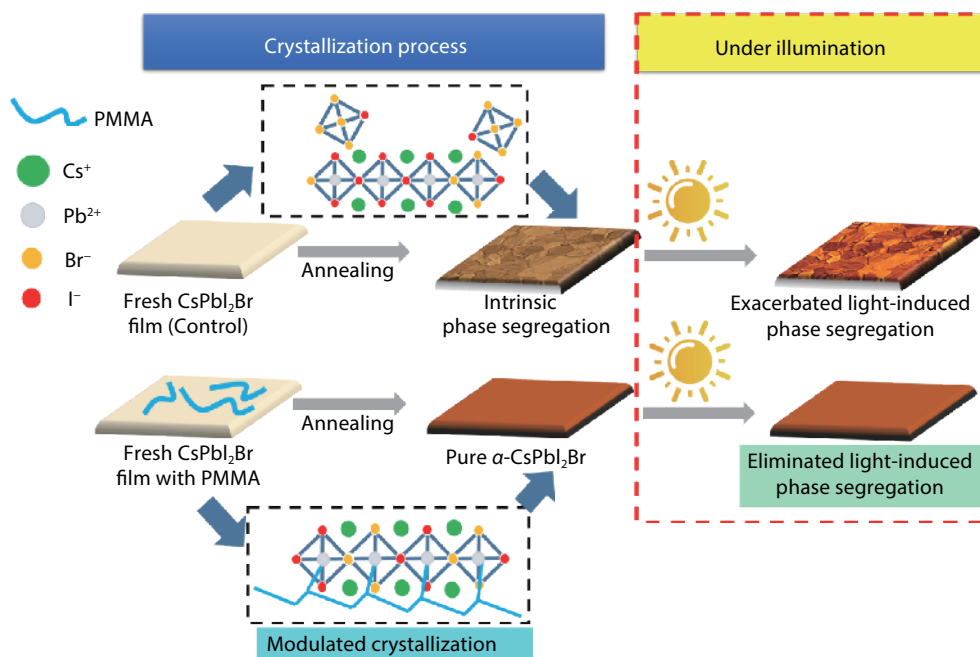


Fig. 2. (Color online) The proposed mechanism for the elimination of phase segregation in CsPbI<sub>2</sub>Br film by PMMA.

place during the formation of CsPbI<sub>2</sub>Br film, and we call it intrinsic phase segregation. On the one hand, intrinsic phase segregation occurs more easily at low annealing temperature. The best devices we discussed above were all made at 240 °C. However, CsPbI<sub>2</sub>Br PSCs made under 100 °C exhibit more serious degradation of SPO (Fig. S16(b)) and larger hysteresis index (Table S4), indicating more severe phase segregation. Low annealing temperature does not favor the growth of homogeneous inorganic perovskite films, which are commonly made at high temperature. But, with PMMA incorporation, hysteresis and SPO degradation (Fig. S16(c)) were suppressed effectively even at low temperature. On the other hand, insufficient components diffusion could occur at fast crystallization rate, which results in phase segregation eventually. Usually, perovskite precursors with DMF solvent exhibit fast crystallization rate, while DMSO could slow down the crystallization<sup>[24]</sup>. When using DMF/DMSO mixed solvent, PL peak split indicates that phase segregation becomes less obvious. PMMA retards the crystallization (Fig. S2), leading to single PL peak, suggesting the elimination of intrinsic phase segregation (Fig. 1(e)).

Light-induced phase segregation is caused by ion migration, and the smaller Br<sup>-</sup> ions are easier to migrate than I<sup>-</sup>. With higher Br content, the phase segregation takes place easily<sup>[25]</sup>. Intrinsic phase segregation generates I-rich phase and Br-rich phase, and this uneven composition will exacerbate phase segregation. According to SEM images (BSE mode) (Fig. S17), more uniform grain color reveals suppressed phase segregation. After 45 min illumination, no PL peak split and GIXRD (200) diffraction peak were observed for CsPbI<sub>2</sub>Br film with PMMA (Fig. 1(f), Fig. S18 and Fig. S19)<sup>[9]</sup>, indicating that light-induced phase segregation was suppressed by PMMA. We further evaluated the photostability of CsPbI<sub>2</sub>Br devices under continuous illumination (unencapsulated in N<sub>2</sub> glovebox). A ~36% PCE drop was observed for the control device after 400 h operation, while for PMMA-containing device, the PCE dropped by ~17% (Fig. S20(b)). The improved photostability

was due to the elimination of phase segregation.

We propose a mechanism for the elimination of phase segregation in CsPbI<sub>2</sub>Br film by using PMMA (Fig. 2). The coordination interactions between C=O groups in PMMA and Pb<sup>2+</sup> in CsPbI<sub>2</sub>Br (Fig. S21 and Fig. S22) lead to lowered crystallization rate, making uniform distribution of I<sup>-</sup> and Br<sup>-</sup> anions<sup>[21]</sup>. The intrinsic phase segregation is eliminated at low annealing temperature and this prohibition effect is expected to exist under light illumination as well, resulting in suppressed *J*-*V* hysteresis and eliminated light-induced phase segregation.

In summary, PMMA was added into CsPbI<sub>2</sub>Br layer to modulate the crystallization and eliminate the phase segregation. PMMA can also passivate the trap states. The CsPbI<sub>2</sub>Br solar cells delivered an enhanced PCE of 15.88% and an improved photostability.

## Acknowledgements

This work was supported by the National Key Research and Development Program of China (2017YFA0402800), National Natural Science Foundation of China (51925206, U1932214), and Collaborative Innovation Program of Hefei Science Center (2020HSC-CIP004). L. Ding thanks the National Key Research and Development Program of China (2017YFA0206600) and the National Natural Science Foundation of China (51773045, 21772030, 51922032, 21961160720) for financial support.

## Appendix A. Supplementary materials

Supplementary materials to this article can be found online at <https://doi.org/10.1088/1674-4926/42/5/050501>.

## References

- [1] Jia X, Zuo C, Tao S, et al. CsPb(I<sub>x</sub>Br<sub>1-x</sub>)<sub>3</sub> solar cells. *Sci Bull*, 2019, 64, 1532
- [2] Hwang T, Lee B, Kim J, et al. From nanostructural evolution to dy-

- namic interplay of constituents: perspectives for perovskite solar cells. *Adv Mater*, 2018, 30, e1704208
- [3] Li M, Liu S, Qiu F, et al. High-efficiency CsPbI<sub>2</sub>Br perovskite solar cells with dopant-free poly(3-hexylthiophene) hole transporting layers. *Adv Energy Mater*, 2020, 10, 2000501
- [4] Shen E, Chen J, Tian Y, et al. Interfacial energy level tuning for efficient and thermostable CsPbI<sub>2</sub>Br perovskite solar cells. *Adv Sci*, 2020, 7, 1901952
- [5] Chen W, Chen H, Xu G, et al. Precise control of crystal growth for highly efficient CsPbI<sub>2</sub>Br perovskite solar cells. *Joule*, 2019, 3, 191
- [6] Duan C, Cui J, Zhang M, et al. Precursor engineering for ambient-compatible antisolvent-free fabrication of high-efficiency CsPbI<sub>2</sub>Br perovskite solar cells. *Adv Energy Mater*, 2020, 10, 2000691
- [7] Han Y, Zhao H, Duan C, et al. Controlled n-doping in air-stable CsPbI<sub>2</sub>Br perovskite solar cells with a record efficiency of 16.79%. *Adv Funct Mater*, 2020, 30, 1909972
- [8] Xiang W, Wang W, Kubicki D, et al. Europium-doped CsPbI<sub>2</sub>Br for stable and highly efficient inorganic perovskite solar cells. *Joule*, 2019, 3, 205
- [9] Wang W, Wang R, Wang Z, et al. Tailored phase transformation of CsPbI<sub>2</sub>Br films by Copper(ii) bromide for high-performance all-inorganic perovskite solar cells. *Nano Lett*, 2019, 19, 5176
- [10] Liu C, Li W, Li H, et al. Structurally reconstructed CsPbI<sub>2</sub>Br perovskite for highly stable and square-centimeter all-inorganic perovskite solar cells. *Adv Energy Mater*, 2019, 9, 1803572
- [11] Zhang T, Li H, Liu S, et al. Low-temperature stable  $\alpha$ -phase inorganic perovskite compounds via crystal cross-linking. *J Phys Chem Lett*, 2019, 10, 200
- [12] Zhao H, Yang S, Han Y, et al. A high mobility conjugated polymer enables air and thermally stable CsPbI<sub>2</sub>Br perovskite solar cells with an efficiency exceeding 15%. *Adv Mater Technol*, 2019, 4, 1900311
- [13] Fu S, Zhang W, Li X, et al. Dual-protection strategy for high-efficiency and stable CsPbI<sub>2</sub>Br inorganic perovskite solar cells. *ACS Energy Lett*, 2020, 5, 676
- [14] Liu C, He J, Wu M, et al. All-inorganic CsPbI<sub>2</sub>Br perovskite solar cell with open-circuit voltage over 1.3 V by balancing electron and hole transport. *Sol RRL*, 2020, 4, 2000016
- [15] Mali S, Patil J, Shinde P, et al. Fully air-processed dynamic hot-air assisted M:CsPbI<sub>2</sub>Br (M: Eu<sup>2+</sup>, In<sup>3+</sup>) for stable inorganic perovskite solar cells. *Matter*, 2021, 4, 1
- [16] Beal R, Slotcavage D, Leijtens T, et al. Cesium lead halide perovskites with improved stability for tandem solar cells. *J Phys Chem Lett*, 2016, 7, 746
- [17] Yan L, Xue Q, Liu M, et al. Interface engineering for all-inorganic CsPbI<sub>2</sub>Br perovskite solar cells with efficiency over 14%. *Adv Mater*, 2018, 30, e1802509
- [18] Tian J, Xue Q, Tang X, et al. Dual interfacial design for efficient CsPbI<sub>2</sub>Br perovskite solar cells with improved photostability. *Adv Mater*, 2019, 31, e1901152
- [19] Xiao Q, Tian J, Xue Q, et al. Squaraine-based polymeric hole-transporting materials with comprehensive passivation effects for efficient all-inorganic perovskite solar cells. *Angew Chem Int Ed*, 2019, 58, 17724
- [20] Zai H, Zhang D, Li L, et al. Low-temperature-processed inorganic perovskite solar cells via solvent engineering with enhanced mass transport. *J Mater Chem A*, 2018, 6, 23602
- [21] Bi D, Yi C, Luo J, et al. Polymer-templated nucleation and crystal growth of perovskite films for solar cells with efficiency greater than 21%. *Nat Energy*, 2016, 1, 16142
- [22] Li B, Zhen J, Wan Y, et al. Anchoring fullerene onto perovskite film via grafting pyridine toward enhanced electron transport in high-efficiency solar cells. *ACS Appl Mater Interfaces*, 2018, 10, 32471
- [23] Wang J, Zhang J, Zhou Y, et al. Highly efficient all-inorganic perovskite solar cells with suppressed non-radiative recombination by a Lewis base. *Nat Commun*, 2020, 11, 177
- [24] Rao H, Ye S, Gu F, et al. Morphology controlling of all-inorganic perovskite at low temperature for efficient rigid and flexible solar cells. *Adv Energy Mater*, 2018, 8, 1800758
- [25] Slotcavage D, Karunadasa H, McGehee M, et al. Light-induced phase segregation in halide-perovskite absorbers. *ACS Energy Lett*, 2016, 1, 1199



**Yanbo Shang** got his BS degree from Dalian University of Technology in 2017. Now he is a PhD student at University of Science and Technology of China under the supervision of Prof. Shangfeng Yang. His work focuses on all-inorganic perovskite solar cells.



**Liming Ding** got his PhD from University of Science and Technology of China (was a joint student at Changchun Institute of Applied Chemistry, CAS). He started his research on OSCs and PLEDs in Olle Inganäs Lab in 1998. Later on, he worked at National Center for Polymer Research, Wright-Patterson Air Force Base and Argonne National Lab (USA). He joined Konarka as a Senior Scientist in 2008. In 2010, he joined National Center for Nanoscience and Technology as a full professor. His research focuses on functional materials and devices.



**Shangfeng Yang** got his PhD from Hong Kong University of Science and Technology in 2003. He then joined Leibniz Institute for Solid State and Materials Research, Dresden, Germany as an Alexander von Humboldt Fellow and a Guest Scientist. In Dec 2007, he joined University of Science and Technology of China as a full professor. His research interests include the synthesis of fullerene-based nanocarbons toward applications in energy devices.